AN INVESTIGATION ON THE CLIMATIC EFFECT OF CONTRAIL CIRRUS

K. N. Liou and S. C. Ou

Department of Meteorology/CARSS
University of Utah
Salt Lake City, Utah 84112

G. Koenig

Geophysics Laboratory
Hanscom Air Force Base
Bedford, Massachusetts 01730

ABSTRACT

High cloud cover in the absence of middle and low clouds for Salt Lake City, Utah, during the period 1949-1982 has been analyzed. A significant increase of the mean annual high cloud cover is evident from 1965 to 1982. This increase appears to coincide with the anomalous jet aircraft traffic increase during that period. Analysis of the annual surface temperature for Salt Lake City shows a noticeable increase on the mean annual basis for the period 1965-1982. We have developed a two-dimensional (2-D) cloud-climate model to investigate the perturbation of high cloud cover on the temperature fields. The model consists of a 2-D climate model and a cloud formation model that are interactive through the radiation program. The cloud covers and radiation budgets at the top of the atmosphere computed from the present model compare reasonably well with observations. A 5% uniform increase in high cloud cover at the latitudes between 20° to 70°N would produce an increase in surface temperature by about 1°K with small variations across the latitudes. The positive surface temperature feedback associated with the high cloud cover increase is due to enhanced infrared emission from the additional high cloud cover and specific humidity produced from the 2-D model.

1. INTRODUCTION

Although evidence of changes in global average cloudiness does not exist at present, there have been reports that localized cloudiness has increased. Machta and Carpenter (1971) reported on secular increases in the amount of high cloud cover in the absence of low or middle clouds at a number of stations in the United States between 1948 and 1970. It has been suggested that there may be a link between this increase in cloudiness and the expansion of jet aircraft flights in the upper troposphere and lower stratosphere (Study of Man's Impact on Climate, 1971).

The exhaust plume of jet aircraft, consisting primarily of water vapor, carbon dioxide and some hydrocarbons, produces so-called contrail cirrus. The water vapor within the plume may undergo homogeneous and/or heterogeneous nucleation processes, upon which ice particles form and grow. Contrails may persist only a short time if the ambient air is very dry. In humid conditions, they may persist for minutes to several hours and spread into linear formations a few kilometers in width and tens of kilometers in length. Carleton and Lamb (1986) have used the high-resolution Defense Meteorological Satellite Program (DMSP) imagery to study the possibility of detecting and documenting the occurrence of jet contrails during the period July-November 1979. Six days were selected during which contrails were also identified by surface observations near Champaign, Illinois (Wendland and Semonin, 1982). Based on Carleton and Lamb's studies, contrails tend to occur relatively frequently and they tend to cluster in groups.

Changnon (1981) has carried out a detailed analysis of the cloud observations, sunshine measurements, surface temperatures, and air traffic data over the northern midwest region during the period 1901-1977. There appears to be a downward trend of the annual number of clear days in general, implying that the frequency of cloud formation has been increasing. In particular, high cloudiness increased over north-central Illinois and Indiana during the period 1951-1976, which approximately corresponds to the period of rapid expansion of air traffic. The exact percentage of increase has not been determined, however. Changnon has also reported that the number of months with moderated temperature, defined as the difference between the monthly average maximum temperature and minimum temperature that is less than normal difference, has been increasing. This trend is consistent with the increase in cloudiness.

The heating effects of cirrus clouds on the surface temperature have been investigated by Cox (1971) and determined to be positive or negative depending on the cirrus cloud emissivity. Manabe (1975) has discussed the effect of contrails on the surface temperature and points out the importance of cirrus blackness on the temperature sensitivity experiment. Freeman and Liou (1979) have investigated the increased effect of contrail cirrus cover in mid-latitudes on the radiative budget of the earth-atmosphere system. Extensive one-dimensional numerical experiments have been carried out by Liou and Gebhart (1982) to study the effects of cirrus clouds on equilibrium temperatures. High cirrus clouds above about 8 km would produce a warming effect at the surface. The degree of the warming is a function of the cirrus cloud optical depth (or emissivity). Ou and Liou (1984) have constructed a 2-D climate model based on the energy balance approach to study the effect of the radiative properties of cirrus clouds on global temperature perturbations. Research efforts pertaining to cirrus clouds and climate have been comprehensively reviewed in Liou (1986).

In this paper, we analyze the high cloudiness and surface temperature in Salt Lake City, Utah, from 1948 to 1982. This is described in Section 2. To understand the impact of the potential increase of high cloudiness on temperature, we have carried out a numerical study using a 2-D climate model developed by Ou and Liou (1984). In

Section 3, we present the basic model and the modifications involving a cloud formation program. Perturbation studies and numerical results are presented in Section 4. Concluding remarks are given in Section 5.

2. TRENDS IN HIGH CLOUDINESS AND SURFACE TEMPERATURE FOR SALT LAKE CITY

We have analyzed the high cloudiness (or cloud amount or cloud cover) for Salt Lake City from 1949 to 1982. The three hourly weather observations reported by the National Weather Service at Salt Lake City International Airport were used to determine the sky cover information. For each observation the cloud amount, in tenths of sky coverage, cloud type and visibility were recorded. When the sky cover is less than one tenth for a particular cloud type, it is reported as zero tenths. As many as four cloud types can be reported on a single observation including Ci (high cloud), Ac (middle cloud), and Sc and Cu (low clouds). The high cloud types encountered were cirrus, cirrostratus, cirrocumulus and cirrocumulus standing lenticular.

The monthly average high cloudiness was computed using only those cases in which the sum of the low and middle cloud amount was 0.5 tenths or less. The monthly average high cloudiness was then used to compute the annual high cloudiness. Based on the results of the student t test, the annual high cloudiness, with no low or middle intervening cloudiness, may be considered as two separate populations. The first group corresponds to the annual high cloudiness for the period from 1949 to 1964, while the second accounts for the period 1965 to 1982, as shown in Fig. 1. The mean high cloud amounts for the first and second time periods are 11.8% and 19.6%, respectively. It is noted that Machta and Carpenter (1971) derived a mean high cloud amount of 19.2% for the time period 1965–1969. The mean high cloud amount for the period 1970-1982 was 19.8%, representing only a slight increase over the 1965-1969 period.

We have computed domestic jet fuel consumption from 1956 to 1982. A significant increase in domestic jet fuel consumption in the mid 60's is evident. However, very little increase was shown during the period 1969-1982 (Fig. 1). The sharp anomalous increase in annual high cloudiness appears to coincide with the significant increase in domestic jet fuel consumption in the mid 60's. In fact, the slopes of the linear fit of the annual high cloudiness for the time periods of 1950-1959, 1960-1969 and 1970-1979 are -0.0048, 0.096 and 0.03, respectively. The sharp increase in the domestic jet fuel consumption during the 1960-1969 time frame appears to suggest a possible causative relationship between domestic jet fuel consumption, i.e., increased jet aircraft traffic, and the increase in annual high cloud amount since 1965. During the 1970-1982 time period the frequency of occurrence of high cloud observations decreased. This suggests that the increase in mean annual high cloud amount was due primarily to an increase in cloud amount. Thus, it appears probable that the increase in the high cloud amount could be linked to the increased jet aircraft traffic.

To investigate the potential effect of the increase in high cloud amount on the

temperature field, we have analyzed the surface temperature data published by the National Climatic Center. The annual surface temperature values for Salt Lake City ov the period 1949-1982 were calculated. The monthly average temperature was obtained by summing the daily maximum and minimum temperatures for the month and dividing by the number of days in the month. The annual surface temperature was obtained by averaging the monthly average temperature information. The temperature data was subdivided into two time periods that coincided with the time periods for high cloud amount, as shown in Fig. 2. The slope for the linear fit of temperature for the first time period is actually negative (-0.032), but the coefficient of determination is fairly small (0.11). This is not the case for the second time period, where the

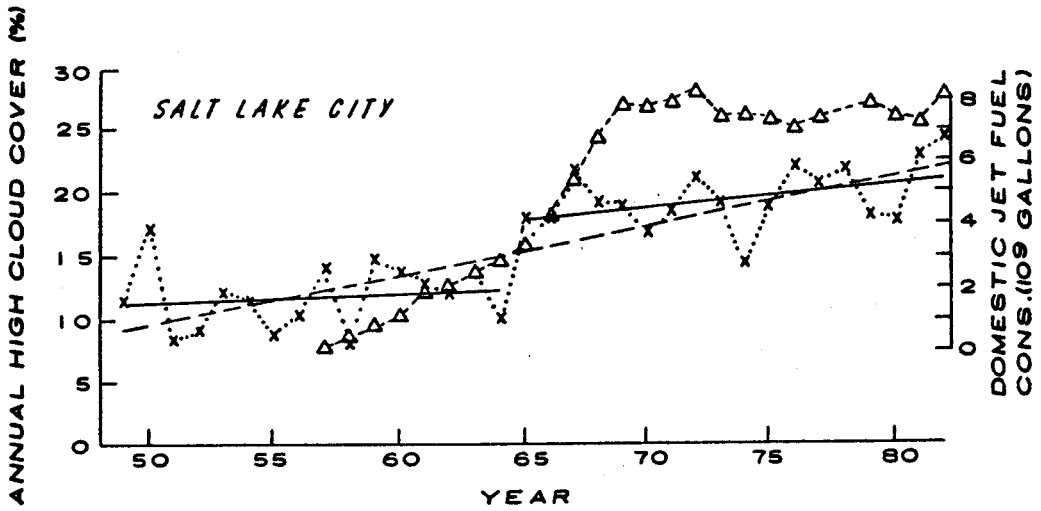

Fig. 1. Mean annual high cloud cover in Salt Lake City from 1948 to 1982 (x) and domestic jet fuel consumption (Δ). The two solid lines are the statistical fitting curves for high cloud cover during the periods 1948-1964 and 1965-1982. The statistical fitting curve for the entire period is denoted by the dashed line.

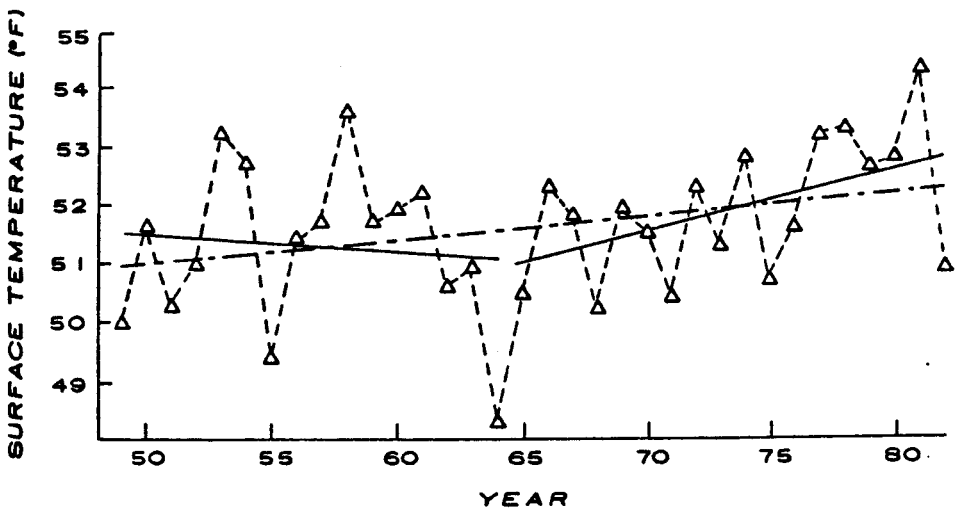

Fig. 2. Mean annual surface temperature in Salt Lake City from 1948 to 1982. The two solid lines are the statistical fitting curves for surface temperature during the periods 1948-1964 and 1965-1982. The statistical fitting curve for the entire period is denoted by the dashed line.

slope is positive (0.107) and the coefficient of determination (0.50) is approximately five times greater than that of the first time period.

An increase in regional surface temperatures could be caused by a number of factors, ranging from natural climatic variabilities to human influence on climate. The correlation between the mean high cloud amounts and mean surface temperatures for the periods 1949–1964 and 1965–1982 appears to suggest that the increase in the surface temperature during the latter period could be related to the increase in high cloud amount.

3. TWO DIMENSIONAL CLOUD-CLIMATE MODEL

To understand the potential effects of high cloud cover variations on the temperature field, we have modified the 2-D climate model developed by Ou and Liou (1984) to perform sensitivity experiments.

a. The 2-D Climate Model

The present 2-D climate model is based on the energy balance between radiative heating and heating produced by horizontal and vertical turbulent transports. The governing equation may be written in the form

$$\frac{\partial}{\partial t}\rho[\bar{E}] + \frac{1}{a\cos\lambda}\frac{\partial}{\partial\lambda}\cos\lambda\, F_h + \frac{\partial F_v}{\partial z} = -\frac{\partial F}{\partial z} \quad , \tag{1}$$

where F_h, F_v and F represent the moist static energy fluxes of horizontal and vertical transports, and the net radiative flux, respectively. They are defined by

$$F_h = \rho([\bar{v}][\bar{E}] + [\overline{v'E'}] + [\overline{v^*E^*}]) \quad , \tag{2}$$

$$F_v = \rho([\bar{w}][\bar{E}] + [\overline{w'E'}] + [\overline{w^*E^*}]) \quad , \tag{3}$$

$$F = F_s(\lambda, z) - F_{IR}(\lambda, z) \quad . \tag{4}$$

In the preceding equations, ρ is the air density, t the time, a the earth radius, λ the latitude, and z the height. The moist static energy, $E = C_pT + gz + Lq$, where C_p is the specific heat at constant pressure, g the gravitational acceleration, L latent heat, and q the specific humidity. v and w are the meridional and vertical wind velocities, respectively, and F_s and F_{IR} the net downward solar and IR fluxes, respectively. The symbol $[\bar{}]$ represents temporal and zonal averages. The terms on the right hand side (r.h.s.) of Eq. (2) denote the transport of moist static energy by mean motions, transient eddies, and stationary eddies in the meridional direction respectively. Likewise, the terms on the r.h.s. of Eq. (3) denote their counterparts in the vertical direction. The vertical stationary eddy is a very small quantity. For

all practical purposes it may be ignored. The vertical transient eddy may be parameterized using the mixing length theory. The mean flow terms depend on the vertical and horizontal velocities, which are prescribed by using the annual zonal data computed by Oort (1983). This implies that the Hadley circulation is fixed in the model. We have used the mixing length theory to parameterize the large-scale horizontal eddy fluxes in a manner described in Ou and Liou (1984).

b. 2-D Cloud-Moisture Model

An equilibrium 2-D cloud-moisture model has been developed for the simulation of zonally averaged specific humidity, cloud liquid water content (LWC), and cloud cover. The governing equations may be written

$$\frac{1}{a\cos\lambda}\frac{\partial}{\partial\lambda}(\cos\lambda\, F_h^q) + \frac{\partial F_v^q}{\partial z} = -\eta\frac{Q_c}{L} + (1-\eta)\frac{E_r}{L} \quad , \tag{5}$$

$$\frac{1}{a\cos\lambda}\frac{\partial}{\partial\lambda}(\cos\lambda\, F_h^{\ell}) + \frac{\partial F_v^{\ell}}{\partial z} = \eta\frac{Q_c}{L} - P \quad , \tag{6}$$

$$\eta = \frac{h - h_o}{1 - h_o} \quad , \tag{7}$$

where the fluxes of horizontal and vertical transports of specific humidity, q, and ud LWC, ℓ, are defined by

$$F_h^q = \rho([\bar{v}]\,[\bar{q}] + [\overline{v'q'}] + [\overline{v^*\bar{q}^*}]) \quad , \tag{8}$$

$$F_v^q = \rho([\bar{w}]\,[\bar{q}] + [\overline{w'q'}] + [\overline{w^*\bar{q}^*}]) \quad , \tag{9}$$

$$F_h^{\ell} = \rho([\bar{v}]\,[\bar{\ell}] + [\overline{v'\ell'}] + [\overline{v^*\bar{\ell}^*}]) \quad , \tag{10}$$

$$F_v^{\ell} = \rho([\bar{w}]\,[\bar{\ell}] + [\overline{w'\ell'}] + [\overline{w^*\bar{\ell}^*}]) \quad . \tag{11}$$

Parameterizations of the fluxes of the horizontal and vertical transports of specific humidity by eddies follow our previous work described in Ou and Liou (1984). Since global data for the vertical and horizontal transports of cloud LWC by eddies are not available, it is assumed that the ratio of the eddy terms for LWC and specific humidity is approximately proportional to the ratio of the mean LWC and specific humidity. The mean velocity fields are prescribed according to the general circulation statistics provided in Oort (1983).

Eqs. (5)-(11), Q_c, E_r and P denote the rate of condensation, evaporation of precipitation, and generation of precipitation, respectively; η is the cloud cover, h

the relative humidity, and h_o the threshold relative humidity. Equation (7) was derived on the basis of the area-weighted relative humidity in which the relative humidity for the cloud area is taken to be unity. The threshold relative humidity is a closing parameter that is required for the calculation of cloud cover. We follow the parameterized equation suggested by Manabe and Wetherald (1967) in the form

$$h_o = h_{os}\,(p/p_s - 0.02)/0.98 \quad , \tag{12}$$

where p is the atmospheric pressure, p_s the surface pressure, and h_{os} the surface threshold relative humidity, which is obtained from the climatological humidity and temperature values at the surface. At $p \simeq 20$ mb, h_o becomes zero. The preceding relative humidity profile was originally proposed for averaged cloudy sky conditions. However, we find that this profile is steeper than the climatological relative humidity profile. Consequently, by using Eq. (12) for clear sky, the averaged cloudy sky relative humidity will be closer to climatological values. It should be noted that the only prescribed value in the model is h_{os}, which is for clear conditions only, and that the model allows clouds to form above the second model layer from the surface.

The derivation of an analytic expression for the rate of condensation, Q_c, requires knowledge of the vertical velocity in the cloudy region. We first define the in-cloud vertical flux of saturation specific humidity, q_s, as $\rho w_s q_s$, where w_s is the in-cloud vertical velocity. Based on the energy conservation principle, Q_c must be proportional to the divergence of $\rho w_s q_s L$. Thus we have

$$\frac{Q_c}{L} = -\frac{\partial}{\partial z}\,(\rho\, w_s\, q_s) \quad . \tag{13}$$

The in-cloud vertical velocity is an unknown parameter. To obtain Q_c, another independent equation is required. Based on the Richardson equation (see, e.g., Dutton 1976), we have

$$\frac{Q_c}{LC_p} = F_h^T + \frac{w_s}{1-\eta}\,\frac{\partial[\bar{T}]}{\partial z} + \gamma_d \quad , \tag{14}$$

where γ_d is the adiabatic lapse rate, and the flux of the horizontal transport of sensible heat in 2-D space is defined by

$$F_h^T = \frac{1}{a\cos\lambda}\,\frac{\partial}{\partial\lambda}\,\{\cos\lambda\,([\bar{v}]\,[\bar{T}] + [\overline{v'T'}] + [\overline{v^*\,T^*}])\} \quad . \tag{15}$$

If $F_h^T < 0$, heating will be produced due to horizontal convergence. However, if $F_h^T > 0$, cooling will be produced. Parameterizations of the fluxes of the horizontal and vertical transports of sensible heat follow the work described in Ou and Liou (1984).

In Eq. (5) the evaporation term associated with precipitation at a given level must be

related to the grid-averaged total downward precipitation flux reaching that level and the difference between the specific humidity in the clear column and its saturation lue. Thus we have

$$\frac{E_r(z)}{L} = k_r \rho(q_s - q_o) \tilde{P}(z) \quad , \tag{16}$$

where $k_r = 1.44\ cm^2\ g^{-1}$, which is derived from known microphysical constants, and

$$\tilde{P}(z) = \int_z^{z_t} [\rho\eta P(z') - (1-\eta) E_r(z')/L]dz' \quad , \tag{17}$$

where z_t is the cloud top height. Equation (17) represents the accumulated balance between the rates of generation and evaporation of precipitation. Furthermore, the rate of generation of precipitation can be parameterized in terms of the so-called auto-conversion factor and cloud LWC mixing ratio in the form (Ogura and Takahashi, 1971; Sundqvist, 1978)

$$P(z) = \eta\rho\, c_o \ell_c [1-\exp(-\ell_o^2/\ell_r^2)] \quad , \tag{18}$$

where $c_o = 10^{-4}\ s^{-1}$ is a coefficient representing the time scale required for cloud particles to become precipitation, and $\ell_r = 5 \times 10^{-4}$ is the mean LWC mixing ratio in precipitation clouds.

uations (5), (6) and (14) are three partial differential equations consisting of three unknowns: q, ℓ and $\rho w_s q_s$. The solutions of these equations require appropriate boundary conditions. At the surface ($z=0$), the cloud cover $\eta=0$, so that $q(0) = q_s(T_o)$ h_o, where T_o is the surface temperature and h_o the surface threshold relative humidity. Also, since clouds are not allowed to form at the surface, we have $\ell(0)=0$. The divergence of the in-cloud vertical flux of saturation specific humidity, $\rho w_s q_s$, must be balanced by the surface evaporation and horizontal convergence of moist sources by mean motions and eddies that are parameterized, as described previously. Equations (5), (6), (7), (13), (14), (16) and (18) can then be used to solve for the following variables: q, η, ℓ, P, E_r, Q_c and $\rho w_s q_s$. Once the clouds are formed in model layers, we perform statistical averages to obtain cloud cover and LWC for high, middle and low clouds using the procedures developed by Liou et al. (1985).

c. Radiative Transfer Model

We have used the radiative transfer parameterization program developed by Liou and Ou (1983) and Ou and Liou (1984) in the present study. For infrared radiative transfer, a broadband flux emissivity approach is employed. The entire infrared spectrum is divided into five bands: three for H_2O, one for CO_2, and one for O_3 absorption. The ' x emissivity is expressed in terms of a polynomial function of the pressure and temperature corrected path length for H_2O and O_3 based on band-by-band calculations.

For the CO_2 15 μm band, the flux emissivity is parameterized based on the transmittance values derived from line-by-line integrations according to the procedures developed by Ou and Liou (1983). The broadband infrared emissivity, reflectivity, and transmissivity for high clouds are prescribed as functions of the vertically integrated LWC following the parameterization equations developed by Liou and Wittman (1979). Middle and low cloud types are treated as blackbodies in the infrared.

For solar radiative transfer, the spectrum is divided into 25 bands: six for H_2O, one for CO_2 (which overlaps the H_2O 2.7 μm band), and 18 for O_3. The absorptivities for the H_2O and CO_2 bands are calculated according to the method developed in Liou and Sasamori (1975). For O_3, the band absorptivities are computed using the absorption coefficient values complied by Howard et al. (1961). The clear-sky fluxes are determined from known values of the solar zenith angle and absorptivity. For the cloudy case, the broadband solar reflection and transmission values for various cloud types are obtained from parameterized polynomial functions of the integrated cloud LWC and solar zenith angle provided in Liou and Wittman (1979). The net fluxes above and below clouds are then determined based on the functional values of gaseous absorptivities and the cloud radiative properties by means of an interactive procedure that accounts for the effects of cloud-cloud and cloud-surface multiple reflections.

4. EFFECTS OF CONTRAIL CIRRUS ON CLOUD FORMATION, RADIATION BUDGET AND TEMPERATURE

The present 2-D cloud-climate model is a global model that covers both the Northern and Southern Hemispheres. The latitude-height domain is divided into 16 latitudinal belts. There are fourteen 10° belts between 70°S and 70°N and two 20° belts at the poles. The height coordinate consists of 17 layers, including four 50 mb layers between the surface (~ 1000 mb) and 800 mb, seven 100 mb layers between 800 and 100 mb, and six equally divided layers between 100 and 0.1 mb (top level) on the logarithmic scale.

Although the present model consists of two separate models, they are interactive through the radiation program. First, the climatological temperature field is used to drive the cloud model from which cloud covers and LWCs for high, middle and low cloud types are computed. Using the computed cloud data, radiative heating in the atmosphere and surface radiative fluxes are then computed and incorporated in the climate model to obtain the temperature field. The computed temperature field is subsequently fed back to the radiation program and cloud model. Iterations are carried out until the equilibrium state is reached. Generally, only two to three iterations are required.

In the climate model, we use climatological pressure, and air and O_3 densities. The CO_2 concentration is fixed at 330 ppm. Except for the O_3 density, which is taken from values tabulated in McClatchey et al. (1971), all other climatological profiles are taken from data compiled by Oort (1983). The solar constant and duration of sunlight used are 1360 W/m^2 and 12 h (for annual case). The solar zenith angle varies with latitude and can be computed from the equation relating this angle, latitude, sola

declination and hour angle. The relative humidity is fixed in the climate model. Thus, the humidity feedback due to temperature perturbations is implicitly included in a model. The surface albedo parameterization has been described in Ou and Liou (1984) and will not be repeated here. This parameterization allows the ice-albedo feedback to occur in the model. Because of the complexity of dynamic transport feedback when the cloud model is interactive with the climate model, this feedback is not considered in the present perturbation study. For this reason, temperature perturbations take place at latitudes where contrail cirrus cover is varied.

a. Control Run

The cloud-climate model is first tuned to the present climate state in terms of the temperature field. Using the procedure developed in Ou and Liou (1984), the model computed temperatures are adjusted to within 0.1°K accuracy of climatological temperatures. Figure 3(a)-(d) show the latitudinal distributions of high, middle, low and total cloud covers computed from the model and climatolology. The climatological cloud values are computed from those derived by London (1957) for the Northern Hemisphere and by Sasamori et al. (1972) for the Southern Hemisphere. Six cloud types were listed by these authors. We have grouped them into high, middle and low cloud types according to the procedure outlined in Liou et al. (1985). In general, the model

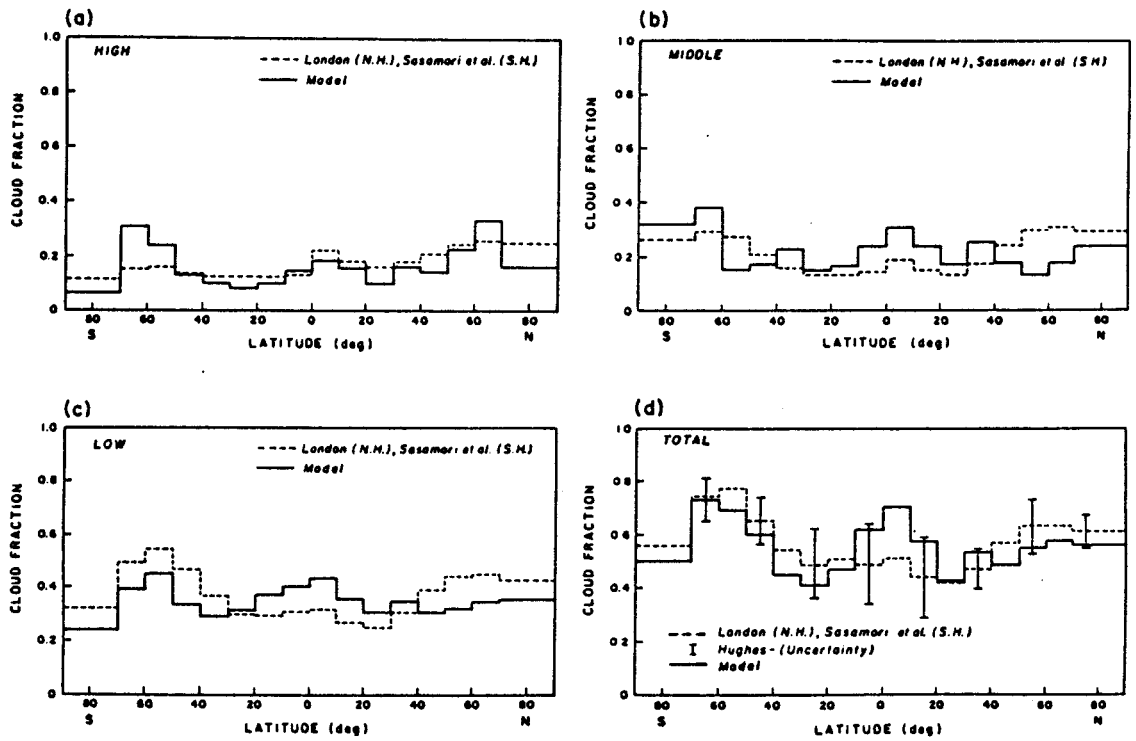

Fig. 3. Latitudinal distributions of high (a), middle (b), low (c), and total (d) cloud covers computed from the present cloud-climate model. Comparisons are made with the cloud covers derived from observed climatological data presented by London (1957) for the Northern Hemisphere and by Sasamori et al. (1972) for the Southern Hemisphere.

produces reasonable cloud cover distributions. High, middle and low cloud covers vary within the range (0.3, 0.1), (0.4, 0.15) and (0.45, 0.25), respectively. Maximum cloud covers ranging from 50-70% are seen in the tropics and mid-latitude storm track regions. In the sub-tropical regions, minimum cloud covers are on the order of 40%. Differences between the model cloud covers and climatological values are generally less than 10%. The best agreement appears to be in mid-latitudes between 30°-60°, where more surface observations were available in the climatological analysis. In the tropics, the model total cloud cover is higher than the climatology indicates. In Fig. 3(d), we have depicted the uncertainty in total cloud cover observations presented by Hughes (1984). It is quite encouraging that the present cloud-climate model produces total cloud covers that are within the observational uncertainty.

Next, we compared the model computed radiation budgets at the top of the atmosphere (TOA) with results derived from satellite observations (Stephens et al., 1981). In Fig. 4, the IR fluxes at TOA are shown (left graph). IR fluxes decrease with increasing latitude, except in the tropics, where convective tower cumulus occur. The model computed IR fluxes in the tropics are higher than observed values. This is due to the fact that the present model does not generate cumulus towers that contain large LWCs. A large difference also occurs in the South Pole regions where the temperature profiles have a large uncertainty. In general, the model IR fluxes are within about 10 W/m^2 of the observed values. Absorbed solar fluxes also compare reasonably well with observations, except in the tropics and Arctic regions (right graph). The latter discrepancies may be due to the solar zenith angle and surface conditions used in model calculations. A number of perturbation experiments were performed to investigate the effects of increasing contrail cirrus in mid-latitudes on the temperature field.

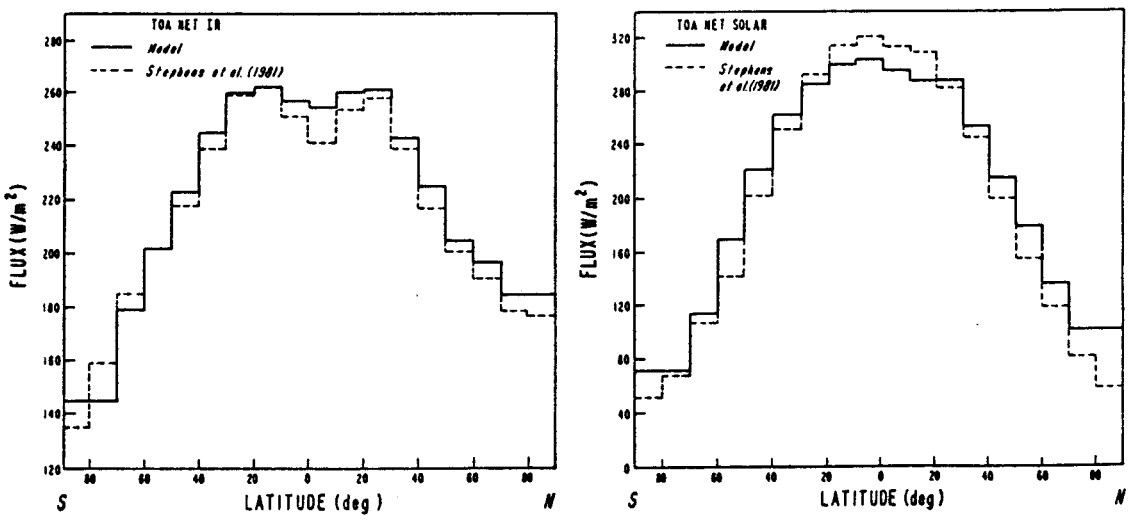

Fig. 4. Latitudinal distributions of net IR flux (left diagram) and net solar flux (right diagram) at the top of the atmosphere computed from the present cloud-climate model. Comparisons are made with satellite derived radiation budgets presented by Stephens et al. (1981).

b. Contrail Cirrus Perturbation Study

performed numerical experiments to investigate the effect of the increase in contrail cirrus cover on cloud formation and temperature fields. Contrail cirrus cover is increased between 20° to 70°N, roughly corresponding to jet aircraft traffic. Three experiments were carried out, including (1) a 5% increase of high cloud cover with all cloud covers and LWCs fixed in the model (C1); (2) a 5% increase of high cloud cover with interactive cloud covers and LWCs generated from the model (C2); and (3) the same experiment as in (2), except with a 10% increase in high cloud cover (C3). To simplify the perturbation study, the radiative properties of contrail cirrus are assumed to be the same as those of high clouds (Ou and Liou, 1984).

The left graph in Fig. 5 shows the changes in high cloud cover for the region between 20° and 70°N. For C1, high cloud cover is increased by 5% across the latitude, as they are fixed in the numerical experiment. However, for C2, high cloud cover increases by more than 5%, except in the 60-70°N latitude belt. The additional 5% high cloud cover causes both specific humidity and temperature to increase in the atmosphere. The increase in specific humidity is greater in the tropics than in mid-latitudes. Thus, the relative humidity increases more in the tropics, leading to the increase in cloud cover, which is directly calculated from the threshold relative humidity method. Similar results have also been obtained from the perturbation experiment involving doubling of CO_2 concentrations (Ou and Liou, 1987). For an increase in high cloud ver of 10%, the high cloud cover increase would be amplified to a value of about 30% in 20-40°N latitudinal belts as a result of the humidity feedback in the present cloud-

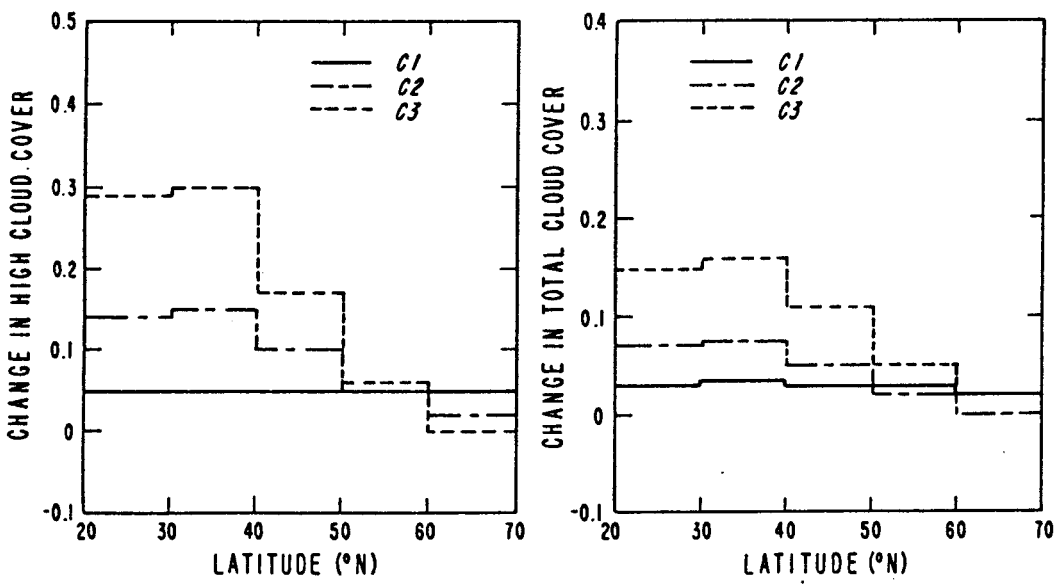

Fig. 5. Changes in high cloud cover (left diagram) and total cloud cover (right diagram) due to the addition of contrail cirrus for the region between 20 and 70°N. C1 denotes a 5% increase in high cloud cover with fixed cloud parameters. C2 denotes a 5% increase in high cloud cover using an interactive cloud program. C3 is the same as C2, except for a 10% increase.

climate model. In terms of the total cloud cover, the increase is less than 5% in the C1 experiment because of cloud overlap effects. In the cases of C2 and C3, increases in the total cloud cover generally mirror those in high cloud cover, except that the magnitudes are smaller due to cloud overlap adjustments.

Changes in atmospheric temperatures for the three perturbation cases are illustrated in Fig. 6. For C1, larger temperature increases of ~6°K at high latitudes are due to the surface albedo feedback included in the model. The amount of temperature increase generally decreases with height. In the case of interactive clouds, the surface albedo feedback effect is substantially reduced. The temperature increase in the C2 case is much smaller than that in C1. Moreover, the maximum temperature increase shifts toward lower latitudes. In Fig. 5, we show that a 5% increase in high cloud cover leads to a substantial amplification in high cloud cover increase (~15%) at 20-40°N, caused by the increase in specific humidity. Enchanced downward thermal infrared emission from additional high clouds is the reason for the temperature increase in the troposphere of low latitudes (IR greenhouse effect). In the cloud perturbation study, low and middle clouds are also increased slightly because of the additional moisture supply. The reduction in the amount of temperature increase in the C2 case is in part due to the increases in low and middle cloud covers (solar albedo effect). In the C3 case, atmospheric temperatures increase more because more high clouds are allowed to form at 20-60°N latitudes. Stratospheric temperatures are only affected slightly due to the high cloud cover increase that occurs in the upper troposphere.

The surface temperature changes produced by the increase of high cloud cover are shown in Fig. 7. In all three cases, surface temperatures increase across the latitudes where cloud cover perturbations take place. For C1, in which clouds are fixed in the model, surface temperature increases from 2 to 6°K with the largest increase occuring at 60-70°N. The surface albedo feedback is the primary reason for this increase, as pointed out previously. When the cloud formation is interactive in the model (C2), the

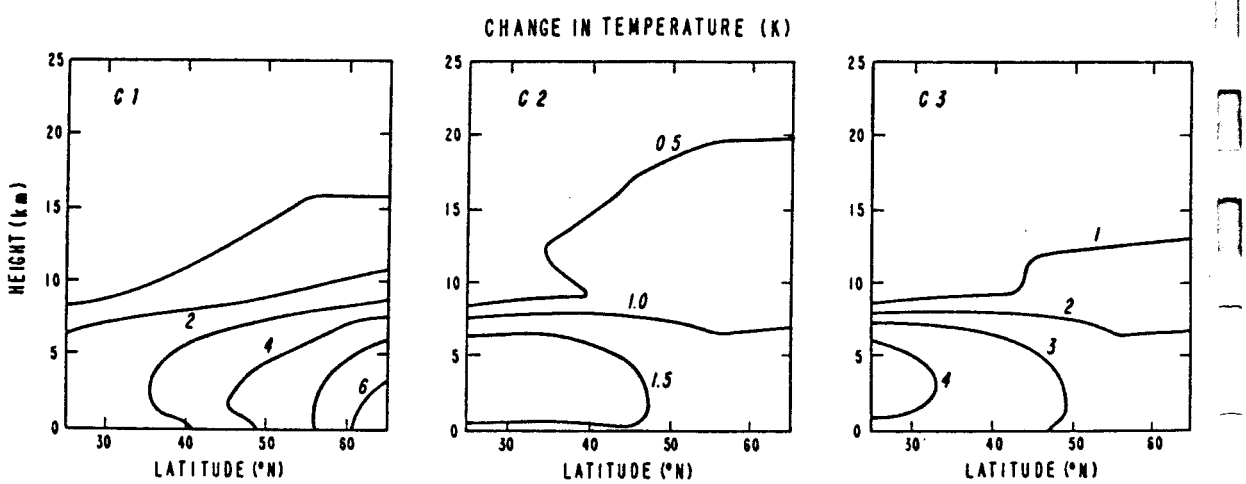

Fig. 6. Changes in atmospheric temperatures due to the increase in high cloud cover for the three cases (C1, C2 and C3) defined in Fig. 5.

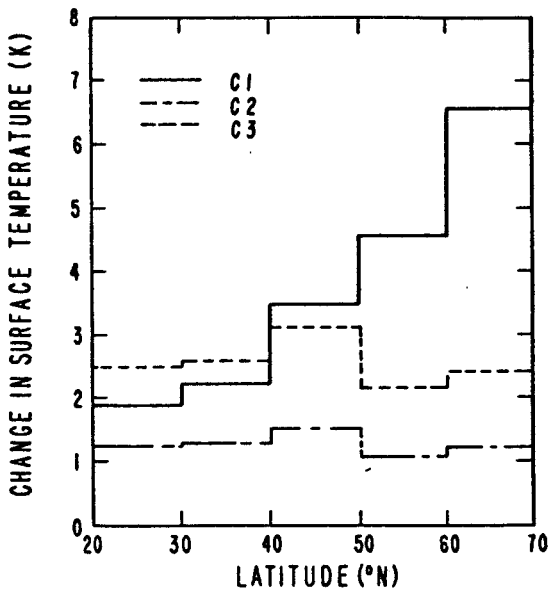

Fig. 7. Changes in surface temperature due to the increase in high cloud cover for the three cases (C1, C2 and C3) defined in Fig. 5.

surface temperature increase is about 1°K but varies with latitude. The decrease in the sensitivity of surface temperature is due to the reduction of surface albedo feedback. In the C3 case, a surface temperature increase of about 2.5°K is obtained because a 10% increase of high cloud cover is used in the perturbation.

In summary, all perturbation experiments involving the increase of high cloud cover reveal increases in atmospheric and surface temperatures. These increases are caused by a positive greenhouse feedback from high cloud cover and specific humidity.

5. CONCLUDING REMARKS

In this paper, we have analyzed high cloud cover in the absence of middle and low clouds for Salt Lake City, Utah, during the period 1949-1982. Based on statistical analyses, the annual high cloud cover may be considered as two separate populations corresponding to the periods 1949-1964 and 1965-1982. A significant increase of mean high cloud cover is evident for the latter period. This increase appears to coincide with the anomalous jet aircraft increase in the mid 60's. An analysis of the mean annual surface temperature for Salt Lake City indicates that the temperature record may also be divided into two groups according to the high cloud cover data. During the period 1965-1982, there is a noticeable temperature increase on the mean annual basis. Factors that could contribute to the increase in regional surface temperatures would be numerous.

The correlation between mean annual high cloud cover and surface temperature in Salt Lake City appears to suggest that the increase in the annual surface temperature during the period 1965-1982 could be caused by the high cloud cover increase associated with jet aircraft traffic during that period.

We have developed a 2-D cloud-climate model to perform sensitivity experiments to understand the perturbation of high cloud cover on cloud-radiation and temperature fields. This model consists of a 2-D climate model and an interactive cloud model that generates cloud covers and LWCs based on the thermodynamic principles. These two models are interactive through the radiation program. The cloud covers and radiation budgets at the top of the atmosphere computed from the cloud-climate model compare reasonably well with observations. Perturbation experiments have been carried out by increasing high cloud cover at the latitudes between 20 to 70°N, roughly corresponding to the jet aircraft traffic corridor. A 5% uniform increase in high cloud cover would produce an increase in surface temperature by about 1°K with some variations across the latitudes. The positive surface temperature feedback produced by the high cloud cover increase is due to enhanced IR emission from the additional high cloud cover and increased specific humidity generated from the 2-D cloud-climate model.

ACKNOWLEDGEMENTS

This research has been supported, in part, by the Air Force Office of Scientific Research Grant AFOSR-87-0294, NASA Grant NAG-1050 and NSF Grant ATM88-15712.

REFERENCES

Carleton, A. M., and P. J. Lamb, 1986: Jet contrails and cirrus cloud: A feasibility study employing high-resolution satellite imagery. *Bull. Amer. Meteor. Soc.*, 67, 301-309.

Changnon, S. A., Jr., 1981: Midwestern cloud, sunshine and temperature trends since 1901: Possible evidence of jet contrail effects. *J. Appl. Meteor.*, 20, 496-508.

Cox, S. K., 1971: Cirrus clouds and climate. *J. Atmos. Sci.*, 28, 1513-1515.

Dutton, J. A., 1976: *The Ceaseless Wind*. McGraw-Hill, 579 pp.

Freeman, K. P., and K. N. Liou, 1979: Climate effects of cirrus clouds. *Adv. Geophys.*, 21, Academic Press, 221-234.

Howard, J. N., J. I. F. King, and P. R. Gast, 1961: Thermal radiation. *Handbook of Geophysics*, MacMillan, Chapter 16.

Hughes, N. A., 1984: Global cloud climatologies: A historical review. *J.Clim. Appl. Meteor.*, 23, 724-751.

Liou, K. N., 1986: Influence of cirrus clouds on weather and climate processes: A global perspective. *Mon. Wea. Rev.*, 114, 1167-1199.

Liou, K. N., and T. Sasamori, 1975: On the transfer of solar radiation in aerosol atmospheres. *J. Atmos. Sci.*, 32, 2166-2177.

Liou, K. N., and G. D. Wittman, 1979: Parameterization of the radiative properties of clouds. *J. Atmos. Sci.*, 36, 1261-1273.

Liou, K. N., and K. L. Gebhart, 1982: Numerical experiments on the thermal equilibrium temperature in cirrus cloudy atmospheres. *J. Meteor. Soc. Japan*, 60, 570-582.

Liou, K. N., and S. C. Ou, 1983: Theory of equilibrium temperatures in radiative-turbulent atmospheres. *J. Atmos. Sci.*, 40, 214-229.

.ou, K. N., S. C. Ou, and P. J. Lu, 1985: Interactive cloud formation and climatic temperature perturbations. *J. Atmos. Sci.*, 42, 1969-1981.

London, J., 1957: A study of the atmospheric heat balance. New York University, *Final Report*, Contract AF19(122)-166, 99 pp.

Machta, L., and T. Carpenter, 1971: Trends in high cloudiness at Denver and Salt Lake City. *Man's Impact on the Climate* (W. H. Mathews, W. W. Kellogg and G. D. Robinson, Eds.), MIT Press, pp. 410-415.

Manabe, S., 1975: Cloudiness and the radiative convective equilibrium. *The Changing Global Environment* (S.F. Singer, Ed.), Reidel, pp. 175-176.

Manabe, S. and R. T. Wetherald, 1967: Thermal equilibrium of the atmosphere with a given distribution of relative humidity. *J. Atmos. Sci.*, 24, 241-259.

McClatchey, R. A., R. W. Fenn, J. E. A. Selby, F. E. Voltz, and J. S. Garing, 1971: Optical properties of the atmosphere. *AFCRL Environmental Research Papers*, 354, 85 pp.

Ogura, Y., and T. Takahashi, 1971: Numerical simulation of the life cycle of a thunderstorm cell. *Mon. Wea. Rev.*, 99, 895-911.

Oort, A. H., 1983: *Global Atmospheric Circulation Statistics*, 1958-1973. *NOAA Prof. Paper*, 14, U.S. Department of Commerce, 180 pp.

Ou, S. C., and K. N. Liou, 1984: A two-dimensional radiative-turbulent climate model. I: Sensitivity to cirrus radiative properties. *J. Atmos. Sci.*, 41, 2289-2309.

Ou, S. C., and K. N. Liou, 1987: Effects of interactive cloud cover and liquid water content program on climatic temperature perturbations. *Atmospheric Radiation: Progress and Prospects*, China Science Press, Beijing, China, pp. 443-440.

Sasamori, T., J. London, and D. V. Hoyt, 1972: Radiation budget of the Southern Hemisphere. *Meteorology of the Southern Hemisphere. Meteor. Monogr.*, 13, 236 pp.

Study of Man's Impact on Climate, 1971: *Inadvertent Climate Modification.* MIT Press, 308 pp.

Stephens, G. L., G. G. Campbell, and T. H. Vonder Haar, 1981: Earth radiation budgets. *J. Geophys. Res.*, 86, 9739-9760.

Sundqvist, H., 1978: A parameterization scheme for non-convective condensation including prediction of cloud water content. *Quart. J. Roy. Meteor. Soc.*, 104, 677-690.

Wendland, W. M., and R. G. Semonin, 1982: Effects of contrail cirrus on surface weather conditions in the midwest - Phase II. *Illinois State Water Survey Contract Report*, 298, Champaign, 95 pp.